

Strain Gauge-Based Torque Sensor for Orthopedic Surgery Applications

May 2, 2025

Technical Team Members:

Grant Garland, Jackson Green, Joseph Liberatore, Matthew McEwen,

Michael Riley, Logan Wasserman

On my honor as a University student, I have neither given nor received unauthorized aid on this assignment as defined by the Honor Guidelines for Thesis-Related Assignments.

ADVISORS

Dr. Michael Momot, Department of Mechanical Engineering

Dr. Jason Forman, Department of Mechanical Engineering

Dr. Joseph Park, Department of Orthopedic Surgery



Problem Statement

The goal of our Mechanical Engineering Capstone design project was to design and develop an attachment to an orthopedic surgical drill that is capable of relaying bone strength characteristics in real-time. Bone strength and toughness are vital attributes during surgical operations as they allow surgeons to determine the approach that is the most appropriate for a specific surgical fixation. This strategy includes the type of fixation screws used as well as the location at which they are inserted. Bone strength is currently estimated using a process called densitometry. This is found by determining the bone mineral density (BMD), which is the average concentration of minerals per unit area. The amount of X-ray energy that the calcium in the bone absorbs reflects the bone mineral content. This value divided by the volume of the bone estimates BMD, and there is a high correlation between BMD and the strength of a bone. Currently, all techniques for estimating bone density are external through the use of X-rays. The most widely used method is dual energy X-ray absorptiometry (DEXA), but others include single energy X-ray absorptiometry (SXA), quantitative computed tomography (QCT), and radiographic absorptiometry (Fogelman & Blake, 2000). At best, these methods only provide a rough estimate of average bone density based on the X-ray signal intensity throughout the entire cross-section of the bone. By providing an accurate density value of local regions in real-time, the goal of our project was to provide the necessary information for orthopedic surgeons to make better informed decisions during procedures.

If orthopedic surgeons were to have access to real-time bone strength, it could change the way they operate and the post-operative treatment plans. Most elective surgeries for older patients require a DEXA scan to give surgeons more information to better perform procedures, but for other groups of individuals, a DEXA scan is not usually taken (Kushchayeva, 2022).

Currently, when surgeons drill into bone they qualitatively feel and determine whether the bone is dense enough to withstand the force of screws being inserted. There is no quantitative way to inform surgeons where the densest place in the bone is during surgery to place screws. BMD is critical for patients undergoing surgery because poor bone health increases the likelihood of fixation failure. Fixation failure occurs when an implant, such as screws, plates, or rods used to stabilize bones, is unable to maintain the proper positioning or alignment. This risk arises from the dependence of screw fixation strength on the underlying bone quality and strength (Kushchayeva, 2022). With quantitative data, surgeons could better determine the strongest spot of the bone and length of the screw that would be optimal for that specific patient. Furthermore, bone strength could help surgeons make more informed decisions regarding post-operative care. For example, if an older woman has excellent bone density, as determined during surgery, then her recovery time could be less than that of an average woman her age (Kushchayeva, 2022).

Research

Current methods for measuring bone density, such as planar X-rays, DEXA scans, or CT scans, provide estimates of average bone density throughout an entire cross section (Johns Hopkins, n.d). As stated above, while these methods can provide estimates of average bone density through a whole cross section, localized information on bone density would be much more helpful for surgeons. DEXA scans, for example, use radiation to measure calcium and other mineral composition in a specific area of bone. The output of such scans is usually a measurement of BMD. Tests for bone density are conducted for a variety of reasons, such as identifying diseases like osteoporosis and determining fracture risk (NIAMS, n.d.).

Previous research has been conducted to determine bone density in similar ways. For example, a study done at the Mammoth Orthopedic Institute in California created a dual motor drill that calculates bone density and screw pull-out force in real time. Their stated purpose was to determine whether monitoring drill bit torque and depth could be used to estimate bone density, hypothesizing that the calculated drilling energy could determine density and correlate to pull-out force. The results of this study showed that their dual motor drill could accurately calculate density and screw pull-out force, allowing surgeons to make real-time decisions in the operating room in order to prevent complications from the surgical repair (Gilmer & Lang, 2018). This study's proof of concept provided us some insight as to how to progress with our own project. It also showed that it is possible to design and implement a device and method to determine bone characteristics using data acquired from drilling, and that surgeons can use this information in real time to determine the best way to repair a fracture.

Ideation

In the ideation stage, the team individually generated potential concepts that incorporated a wide variety of solutions. Some of these ideas are listed below in Table 1.

Table 1: Concept Generation

Idea	Description
A	Attachment with torque sensor that clamps over existing chuck of drill
B	C-Clamp attachment to the back with wires to the sensor between drill bit and chuck
C	“Ligature” style that attaches to the top of the drill
D	New drill bits that have built in torque sensors
E	Full new drill with magnetic attachment to the back with wireless sensor
F	Put magnets inside the chuck and attach a magnetic sensor to detect the speed.
G	Sensor that attaches to the front of the drill that measures applied force by compression
H	Data is automatically stored in patients’ profiles
I	Device inserts into existing chuck to measure torque and transmits data wirelessly
J	Full drill with built-in torque meter
K	Arm sleeve mounted drill press
L	Colored lights attachment
M	Attachment with flip-up screen
N	Attachment between battery and drill that measures current/voltage being used.

Each idea and some combinations of multiple ideas are shown below in Figures 1-10.

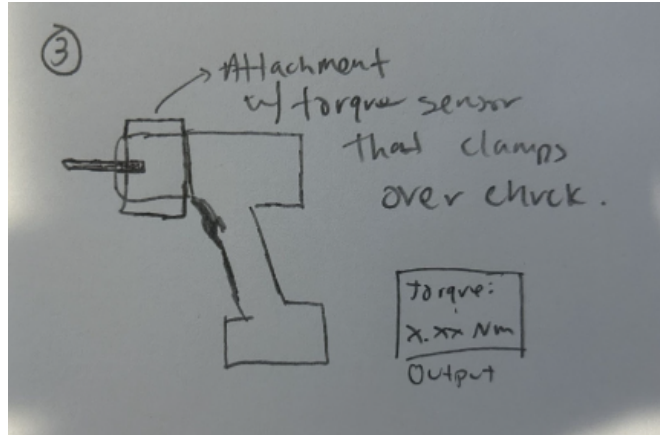


Figure 1: Idea A

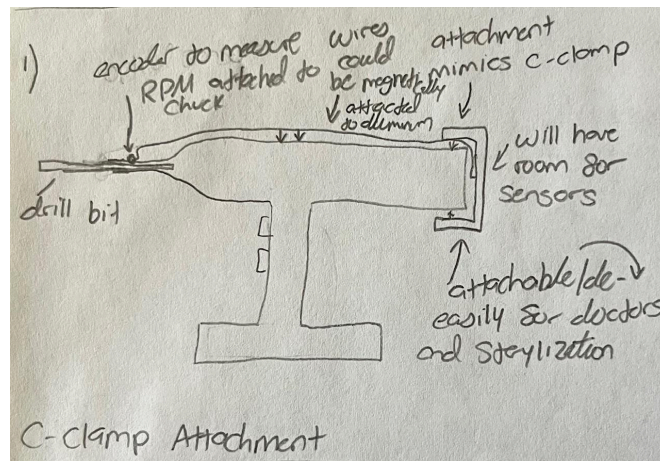


Figure 2: Idea B

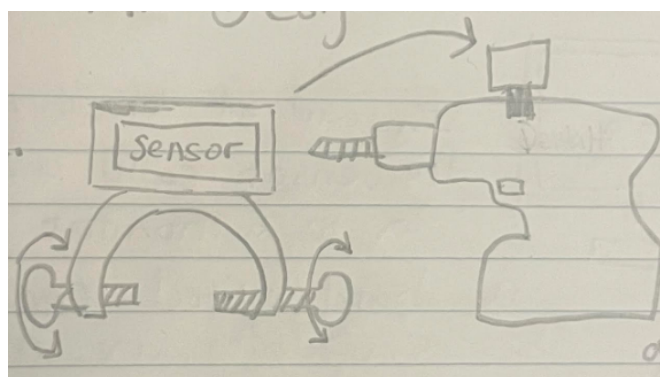


Figure 3: Idea C

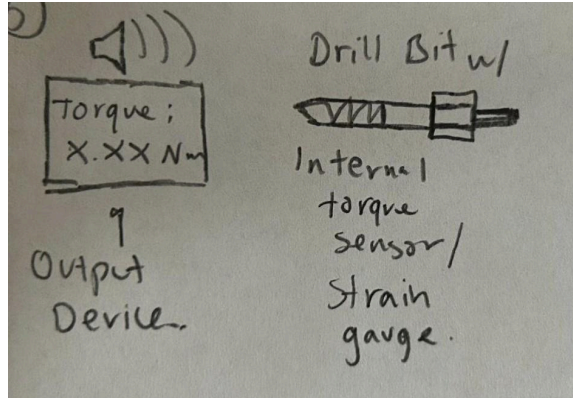


Figure 4: Idea D

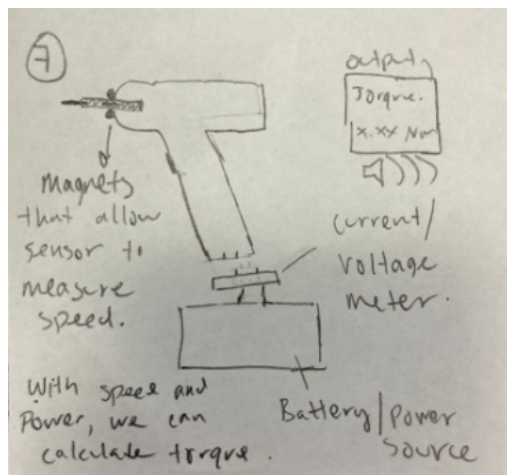


Figure 5: Idea F + N

Drill sends data to computer hard drive for long-term storage



Figure 6: Idea H

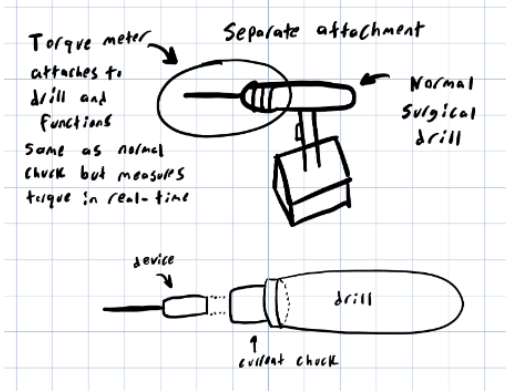


Figure 7: Idea I

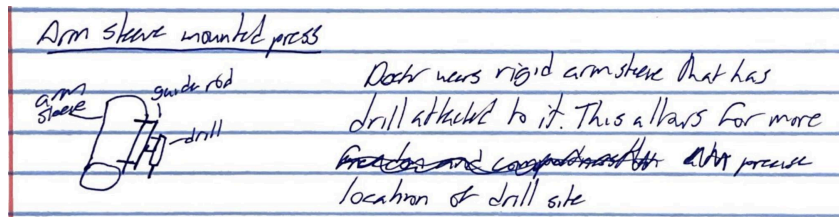


Figure 8: Idea K

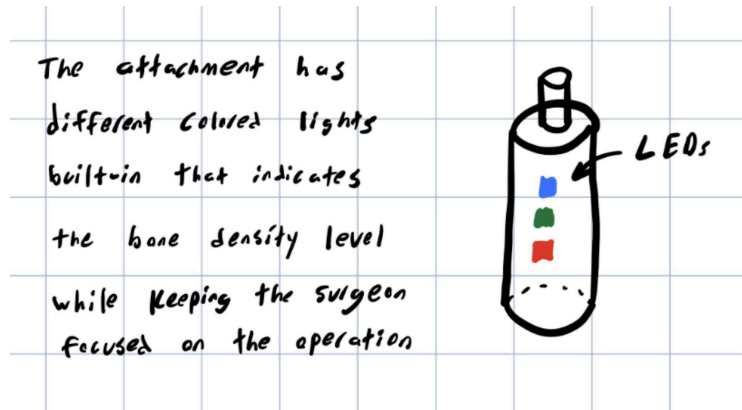


Figure 9: Idea L

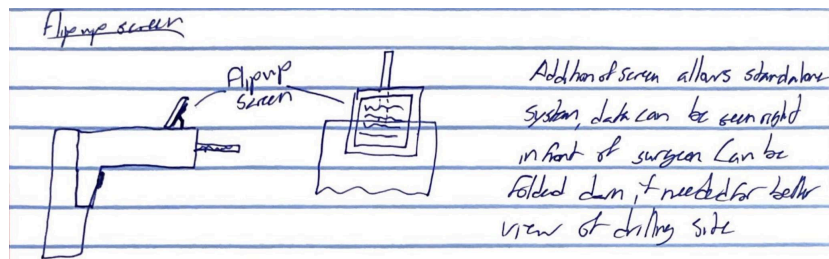


Figure 10: Idea M

Selection and Screening

The spreadsheet that was used for the screening process is shown in Figures 11 and 12.

Each concept was given a score of “positive,” ”negative,” or “neutral” for each selection criteria.

A score of “neutral” meant that the concept was comparable with a standard surgical drill for that selection criteria. A “positive” meant that the selection criteria was better than the reference while a “negative” indicated a worse fit.

Selection Criteria	Concept Variants									
	A: Attachment with torque sensor that clamps over existing chuck of drill	B: C-Clamp attachment to the back with wires to sensor on between drill bit and chuck	C: "Ligature" style that attaches to the top of the drill	D: New drill bits that have built in torque sensors	E: Full new drill with magnetic attachment to the back with wireless sensor	F: Put magnets inside chuck and attach a magnetic sensor to detect the speed	G: Sensor that attaches to front of drill that measures applied force by compression	H: Data is automatically stored long-term in patients' profiles	I: Device inserts into existing chuck to measure torque and transmits data wirelessly	J: Full drill with torque meter built in
Ease of Use	0	-1	-1	1	1	-1	-1	1	1	1
Sterilization	0	-1	1	-1	1	-1	0	0	1	1
Data Readability	0	1	1	1	0	-1	-1	1	1	0
Weight/balance	-1	1	-1	1	-1	1	-1	0	0	0
Ergonomic	1	-1	-1	1	-1	1	1	0	1	0
Resistant to Fluids	0	-1	1	-1	0	0	0	0	-1	0
Cost	0	0	-1	-1	-1	-1	0	1	0	-1
Compatibility with Existing Drills	1	1	1	1	-1	1	-1	0	1	-1
Pluses	2	3	4	5	2	3	1	3	5	2
Sames	5	1	0	0	2	1	3	5	2	4
Minuses	1	4	4	3	4	4	4	0	1	2
Net	1	-1	0	2	-2	-1	-3	3	4	0
Rank	4	9	7	3	12	9	14	2	1	7
Continue?	YES	NO	YES	NO	NO	YES - WITH N	NO	YES	YES	NO

Figure 11: Screening Results for Concepts A-J

	K: arm sleeve mounted drill press	L: Colored lights attachment	M: Attachment with flip up screen	N: Attachment between battery and drill that measures current/voltage being used and relates that to torque	Reference: Existing Surgical Drill
Selection Criteria					
Ease of Use	1	1	1	1	0
Sterilization	-1	0	-1	0	0
Data Readability	0	1	1	0	0
Weight/balance	1	1	-1	0	0
Ergonomic	1	0	0	0	0
Resistant to Fluids	-1	-1	-1	0	0
Cost	-1	0	-1	0	0
Compatibility with Existing Drills	-1	-1	0	0	0
Pluses	3	3	2	1	
Sames	1	3	2	7	
Minuses	4	2	4	0	
Net	-1	1	-2	1	
Rank	9	4	12	4	
Continue?	NO	NO	NO	YES - WITH F	

Figure 12: Screening Results for Concepts K-N and Reference

Our selection criteria were chosen based on the team’s initial specifications for the design. “Ease of use” was a selection criteria due to how important it is for all orthopedic surgeons to be able to operate and understand the device. The ability to sterilize the object is obviously vital as any unsterile objects are harmful and not permitted in the operating room. The ability to read data was chosen as a criteria due to the fact that the device is only practical if the surgeon is able to read the measurements in real-time. Weight and balance were considered due to the fact that these factors are what will allow the surgeon to be accurate and steady while drilling. Ergonomics were considered to ensure that the surgeon would easily be able to apply an axial force while drilling. Because the device will be entering the human body, it must be resistant to fluids. Cost is something that should always be considered, however all of the designs were viewed through the lens of the medical industry and therefore some designs that

may seem expensive for our project were not considered expensive relative to other surgical instruments. The final selection criteria used is the design's compatibility with existing drills. This is important as any design that is not compatible would require the design and production of an entirely new drill.

The scoring spreadsheet that we used to select our design is shown in Figure 13. The four designs that advanced to the scoring process were designs A, C, I, and a hybrid design combining ideas F and N.

Rank out of 5		Concepts							
		A: Attachment with torque sensor that clamps over existing chuck of drill		C: "Ligature" style that attaches to the top of the drill		F: Device inserts into existing chuck to measure torque and transmits data wirelessly		F + N: Attachment between battery and drill that measures current/voltage being used. Uses magnets attached to clamp and magnetic sensor to measure speed with the voltage to measure torque	
Selection Criteria	Weight (%)	Rating	Weighted Score	Rating	Weighted Score	Rating	Weighted Score	Rating	Weighted Score
Ease of Use	15.00%	3	0.45	1	0.15	5	0.75	2	0.3
Sterilization	5.00%	3	0.15	4	0.2	4	0.2	3	0.15
Data Readability	17.50%	3	0.525	5	0.875	3.5	0.6125	3	0.525
Weight/balance	15.00%	2	0.3	1	0.15	3	0.45	3	0.45
Ergonomic	12.50%	4	0.5	2	0.25	4	0.5	4	0.5
Resistant to Fluids	7.50%	3	0.225	4	0.3	2	0.15	3	0.225
Cost	2.50%	3	0.075	2	0.05	3	0.075	1	0.025
Compatibility with Existing Drills	25.00%	5	1.25	5	1.25	5	1.25	2	0.5
Total Score		3.475		3.225		3.9675		2.675	
Rank		2		3		1		4	

Figure 13: Scoring Spreadsheet

Each design was given a score from 1-5 for each selection criteria. That rating was then multiplied by the weight that was assigned to that selection criteria. All of the weighted ratings were then summed for a total score for each design and compared to determine which design was the most promising. As mentioned earlier, compatibility with existing surgical drills was crucial for our designs, therefore this was weighed the most at 25%. Data readability was considered the next most important factor at a weight of 17.5%. The design is not practical if the surgeon is unable to read the results in real-time. Therefore, ease of use and weight/balance were considered the next two important criteria at a weight of 15% as they both play a large role in the surgeon's physical ability to use the device. For the same reason, ergonomics was considered the next most

important selection criterion at a weight of 12.5%. Resistance to fluids and sterilization were given weights of 7.5% and 5% respectively. While these are obviously crucial in the design, the team did not feel that these needed heavy weights due to the fact that these are basically requirements and any feasible design will meet these standards. The least weighted criterion was cost at 2.5%. Due to the high cost of surgical equipment, the cost of this device should not be unreasonable regardless of which design was chosen. At the conclusion of the scoring process, design I was chosen as the design to pursue.

Initial Specifications

After the problem statement was defined, initial specifications were developed as a means of outlining the key requirements of our product. In addition, each specification included a means for measuring them in order to determine if they were attainable. The initial specifications were as follows:

1. The device must be able to accurately estimate local bone characteristics to give a measure of the strength of the bone.
 - a. Measure the density of a human bone using a DEXA scan. Drill 10 different holes into the bone and ensure that the measured density is within 5% of the true density.
2. The device must take real-time measurements.
 - a. The device should update its measurements over a short period of time without a noticeable lapse.
3. The device must be able to be sterilized.
 - a. The device must be able to withstand the heat oven that is currently used to sterilize surgical instruments (270 degrees F).
4. The device must accommodate a range of drill bit sizes.
 - a. The “chuck” or equivalent of the device must be able to open and close enough to accommodate a range of bit sizes. Measure the range of required bit sizes.
5. The device must not decrease the torque of the surgical drill.
 - a. Look up in the user’s manual the maximum torque the drill is supposed to reach. Measure the maximum torque after the device is attached using the device and make sure they are within 2%.

6. The device must be of a reasonable size to not interfere with the surgery.
 - a. The volume of the device is within 10% of current surgical drills.
7. The device must be lightweight enough for surgical use.
 - a. Measure the overall weight/mass of the device and ensure it within 10% of current surgical drills.
8. The device must be ergonomic.
 - a. Survey 5 orthopedic surgeons and have them rate the comfort level on a scale of 1-10, where 1 is extremely uncomfortable and 10 feels like a normal surgical drill (without the device) and ensure the average is above 7.
9. The device must be easy to use.
 - a. Survey 5 orthopedic surgeons and have them rate the ease of use on a scale of 1-10, where 1 is extremely uncomfortable and 10 feels like a normal surgical drill (without the device) and ensure the average is above 7.
10. The device must stay stable throughout use.
 - a. Have surgeons practice with the drill on a material with bone-like characteristics to ensure that it does not rattle during use.
11. The device should be affordable for every hospital/operating room.
 - a. The cost of the device is comparable to similar surgical equipment.
12. The device should remain operational for a prolonged period of time.
 - a. Design the drill to use a battery that is known to go through many charges before the battery maximum capacity deteriorates.
13. The device should be easily attached and removed from the surgical drill.
 - a. Measure the amount of time it takes users to add and remove the device.

14. The device should output the necessary data to something that the surgeon can see or hear in real time.
 - a. Poll surgeons to determine the preferred method of data output (visual, auditory, or neither).
15. The device is capable of saving the data to be reviewed later.
 - a. Ensure the saved output does not lose any data.
16. The device should be durable enough to withstand normal surgical operations.
 - a. Test the device by dropping it from a normal operating table height and ensure it functions properly.
17. The device should be able to be easily maintained/fixable.
 - a. Include an instruction manual and survey surgeon to see if they would be able to fix common problems from instruction manuals.
18. The device must be resistant to fluids commonly found in surgery (blood,water).
 - a. Soak the device in liquid and make sure it maintains its functionality.
19. The device does not damage drill bits over time.
 - a. Measure how worn down the drill bits are and ensure they are consistent without device use.
20. The device should be sensitive to small changes in torque.
 - a. Calibrate the increments so that small differences in bone density are picked up by the device.

These initial specifications served as a guideline for the team to follow throughout the development process by ensuring clarity and context regarding the purpose of the device.

Technical Aspects and Prototypes

The following section outlines the technical development process and key design decisions that led to the creation of our custom torque measurement device. This includes an overview of prototype iterations, component selection, circuit design, and mechanical integration. Each choice was informed by practical constraints, testing outcomes, and the ultimate goal of integrating the system into a surgical drill platform.

Design Evolution

Our original plan was to use an off-the-shelf wireless rotary torque sensor instead of building our own load cell. However, we later discovered that the product we intended to purchase lacked the necessary capabilities and exceeded our budget. As a result, we were forced to pivot to building a custom torque load cell that connects to a Stryker surgical quick connect system. For testing purposes, we modified the end to fit a Jacobs chuck on a standard handheld drill. After pivoting our approach, we created a design that utilized four resistance strain gauges oriented in a Wheatstone Bridge Circuit (Figure 14), a load cell internal structure fabricated out of aluminum, and an electrical system consisting of a microcontroller, load cell amplifier, and battery that allows all of the elements to interact with each other to communicate torque data in real-time.

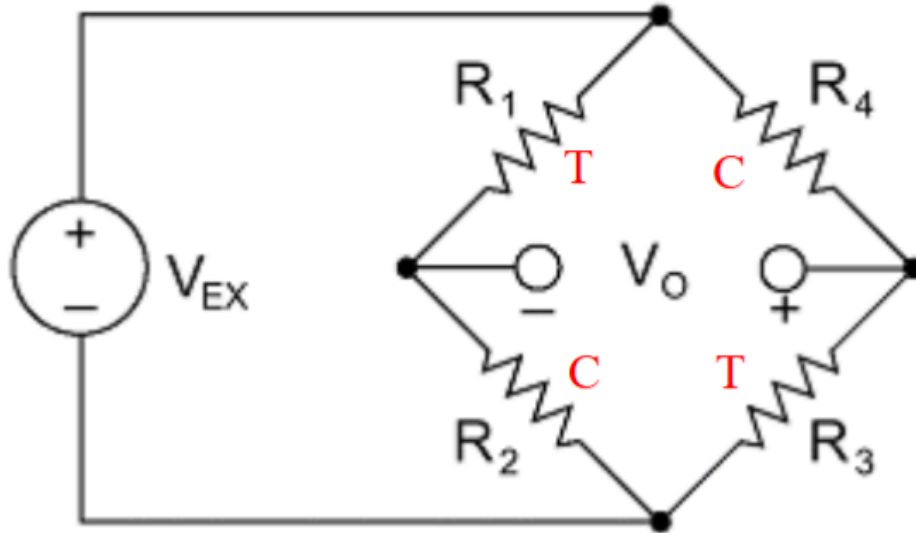


Figure 14: Wheatstone Bridge Circuit. V_{EX} is the excitation voltage, and V_O is the measured output voltage. For full bridge, strain gauges, alternating in compression and tension comprise each of the four resistances. Image from National Instruments (ni.com)

This design evolved significantly over time as further research and testing was conducted. Originally, a slip ring was considered to transfer data off the device to a computer as well as power the device from an external power supply. However, this idea was discarded due to the significant amount of noise that is generated by the slip ring's internal, metal brushes. Therefore, a high-quality slip ring consisting of graphite brushes would have been required to receive a reliable signal, which was outside of the budget provided to us. After discovering this, we decided to pursue using a radio frequency (RF) transmitter for real-time data transmission. Similarly to the slip ring, we had concerns with the validity of the signal using this method due to signal distortions that may occur when this transmitter was rotating at high RPMs. In addition to difficulties getting the RF transmitter to work properly while stationary, this was why we also discarded the idea of using an RF transmitter.

Because of these challenges, we pivoted away from real-time data transmission. We went back to an idea we had early on: using different colored lights to act as an indicator for the strain

and torque level, as seen in Figure 15. Our final design utilizes a single RGB light on-board the device that changes color based on the amount of strain detected. In addition, while this design does not have the real-time data transmission originally desired, it does have the ability to save data for later analysis. Although the final design doesn't have all of the originally intended capabilities, this prototype still serves as a proof of concept that the torque applied via a handheld cordless drill can serve as an indicator for bone strength.

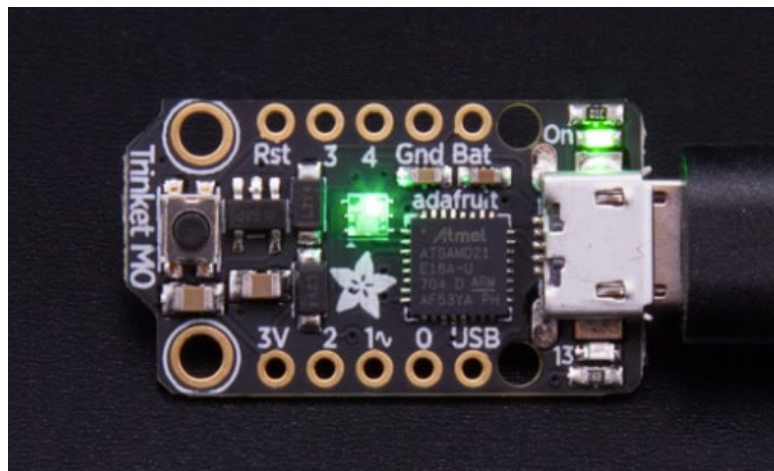


Figure 15: Adafruit Trinket M0 With RGB LED in Center

Initial Testing and Results

Another major consideration was determining the impact that other various forces may have on the torque readings. Therefore, we conducted a series of tests using a Jacobs chuck, digital torque wrench, and weight scale to simultaneously measure peak torque and axial force while drilling into a test specimen under controlled conditions. The testing setup is shown below in Figure 16.



Figure 16: Experimental Setup Consisting of Bathroom Scale (Top Left), RIDGID Handheld Cordless Drill with Precision Torque Wrench Adapter and Square Drive to Jacobs Chuck Adapter (Top Right), and 4x4 Yellow Pine Sample

55 tests were performed using yellow pine with the results between axial force and torque shown in Figure 17. A significant relationship was found, with the torque increasing relatively linearly with increased axial force. Therefore, it is necessary to consider the axial force that the drill operator exerts on the device when computing the relationship between torque and density. The non-zero intercept in the graph likely reflects the baseline torque required to overcome system friction, drill bit engagement, or sensor offset in the absence of applied axial force. An additional 35 tests were performed on a denser wood, maple. A comparison of these two wood varieties shows that the torque required to drill into a material increases with its density.

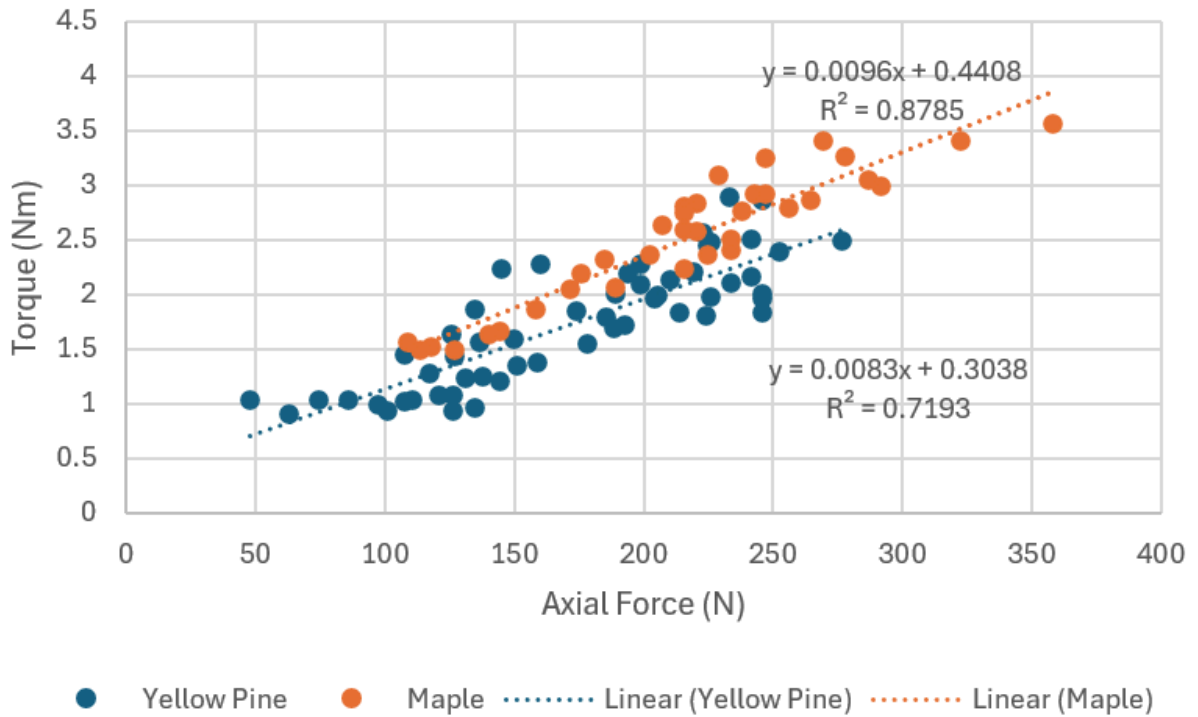


Figure 17: Axial Force (N) vs. Torque (N-m) for Maple and Yellow Pine

Finite Element Analysis

Finite Element Analysis (FEA) was utilized to design the rod that connects the chuck of the drill to the drill bit in the final design. This is where the strain gauges and all of the electronics components are attached as well. When initially designing this part, it was determined that a solid shaft of aluminum would not produce enough measurable strain. Therefore, we decided to remove material from the rod in order to make it more susceptible to torque. Rather than removing material from the inner diameter, which would not impact the results very much, we decided to drill holes throughout the shaft that were perfectly perpendicular to each other. A comparison in maximum strain between a solid aluminum rod and our design is shown below in Figures 18 and 19.



Figure 18: Finite Element Analysis of the Strain for a Solid Load Cell Structure

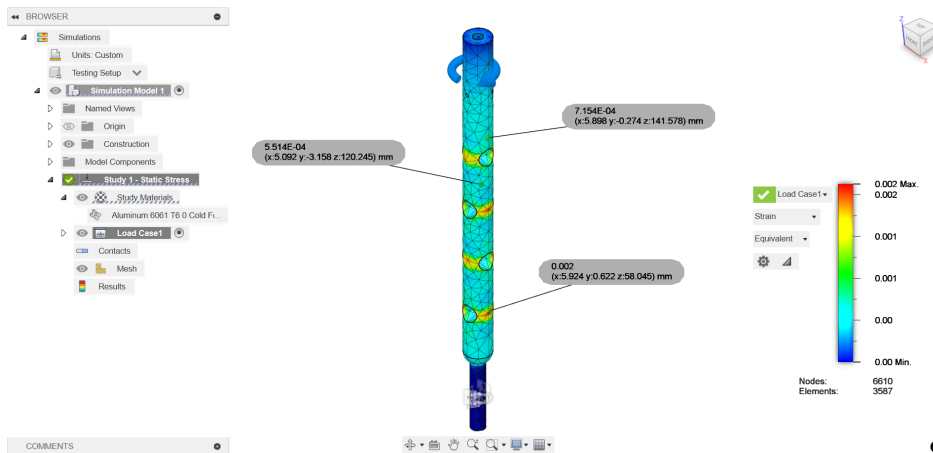


Figure 19: Finite Element Analysis of the Strain for Final Design

Machining the Load Cell

To machine the load cell, we purchased a long, half-inch diameter rod of aluminum from McMaster-Carr. The bandsaw was first used to cut the aluminum to a slightly larger length than the final dimension. In this case, the rod was shortened to roughly 7.5". It was then attached to the lathe so it could be sheared in a more precise manner, reaching the ideal length of 7.36". The rest of the machining was performed on the vertical mill, as it provided extremely accurate

distances for drilling out the material required to put the load cell in the strain range needed. After setting the zero on the edge of the part, the first two thru holes were drilled 3.15" and 5.12" down the shaft. A 5/12" bit was used for drilling as it was the closest empirical bit size to the designed 8 mm hole diameter. The rod was then rotated 90 degrees to drill the other holes 2.17" and 4.13" away from the edge. Similarly, three set screw holes were drilled at 120-degree orientations 1" along the rod, using a 1/16" drill bit. Finally, three flats, roughly 0.79" long, were machined starting from the opposite end. After finishing the part, compatibility with a standard Jacobs chuck was checked. The final load cell with strain gauges attached is shown in Figure 20 below.

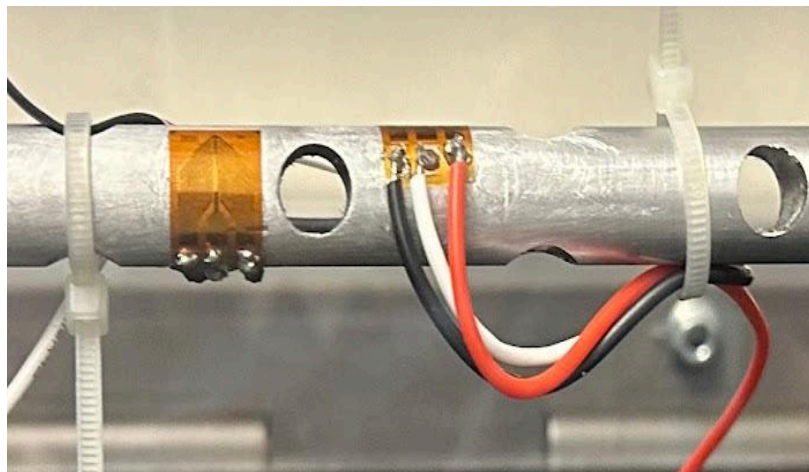


Figure 20: Two Rosette Strain Gauges on Load Cell

Initial Instron Testing

The goal of our initial Instron testing was to establish a quantitative relationship between the applied torque and the resulting strain measured by the strain gauges using an Instron Torsion Machine. Due to the non-uniform and non-homogenous nature of our load cell, it was not feasible to rely solely on theoretical models to determine torque from strain. Therefore, an empirical approach was adopted to characterize this relationship through testing. The strain gauges were configured in a full Wheatstone bridge circuit assembled on a breadboard and

interfaced with a National Instruments Data Acquisition unit using the appropriate full-bridge pinouts. Data acquisition was performed using LabVIEW, with measurements recorded and exported as CSV files for post-processing. The Instron Torsion Machine was programmed to apply torque in a linear ramp to a predefined target value. As illustrated in Figure 21, the measured strain exhibited a clear peak corresponding to the maximum applied torque. Simultaneously, torque-versus-time data was recorded directly from the Instron system. By synchronizing this data with the recorded strain measurements, an initial empirical relationship between torque and strain was established.

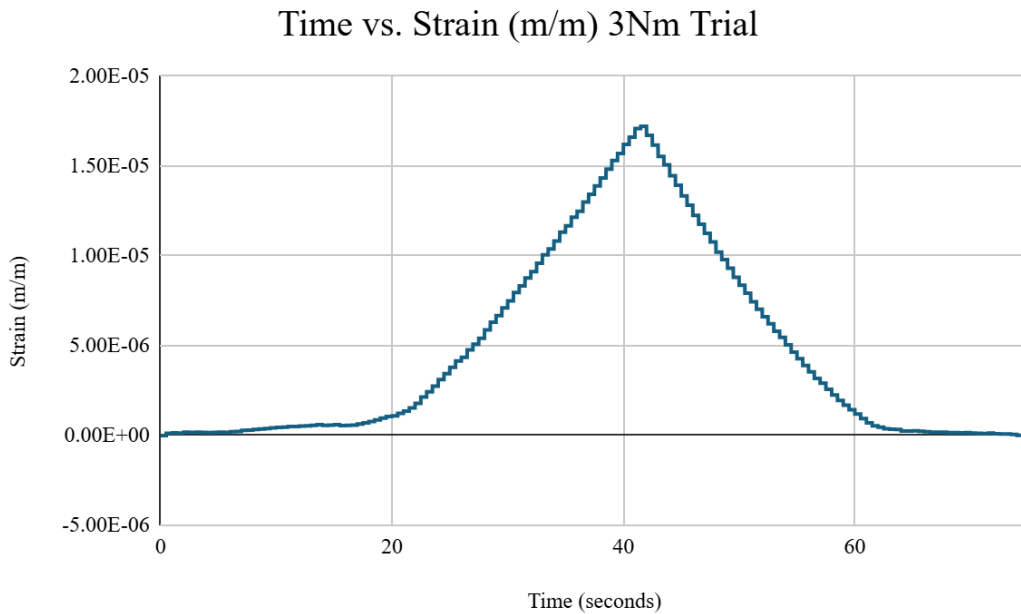


Figure 21: Strain (m/m) vs Time (s) - 3 N-m Trial

Circuit and Diagram

The current prototype consists of five primary components mounted to the load cell using custom-designed 3D-printed collars. Central to the system are two 90-degree Rosette strain gauges affixed directly to the load cell to measure the strain induced by applied torque. These

gauges interface with the HX711 Load Cell Amplifier, an integrated circuit that incorporates a full Wheatstone bridge and amplifies the microvolt-level signals produced by the strain into a range suitable for digital processing. This amplified signal is then transmitted to the Adafruit Trinket M0, which functions as the central processing unit of the system. The Trinket is responsible for acquiring the strain data, operating the onboard status LED, and logging measurements to a CSV file for later analysis. The full circuit is shown below in Figure 22, and the final implementation of the Python program used to control the microcontroller is provided in Appendix C. Power to the system is supplied either through a micro-USB connection or a rechargeable lithium polymer battery. The Adafruit LiPoly Backpack module is employed to facilitate automatic switching between power sources and to manage battery recharging when connected to a computer. Although the current configuration remains a proof of concept, the system successfully demonstrates core functionality and serves as a robust platform for future refinement and integration into a fully operational surgical drill assembly.

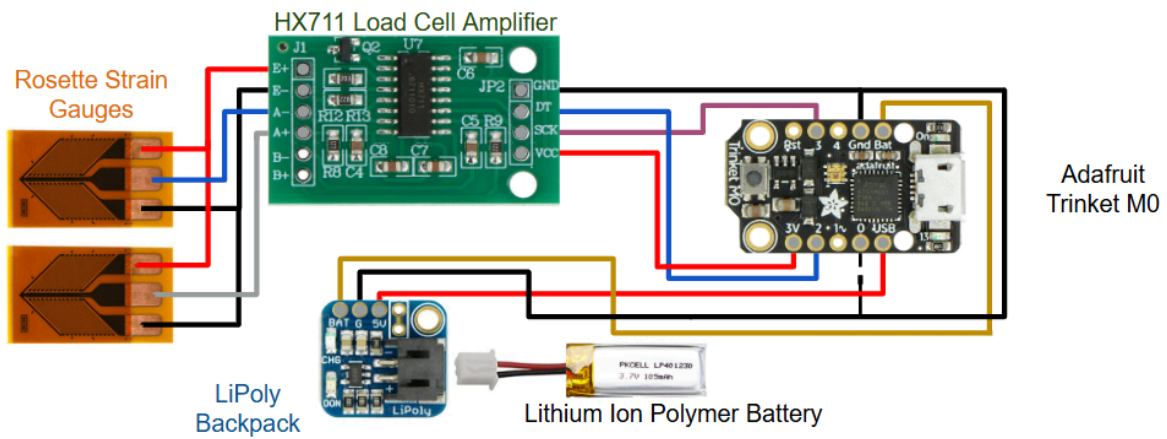


Figure 22: Circuit Diagram

Testing

Final Instron Testing

After assembling all of the electronic components, we went back to the Instron Torsion machine to obtain a more accurate relationship between the torque and strain. Now that we had an amplifier, we would be able to see smaller changes in the strain more accurately. We performed the same procedure as the previous Instron testing where we took 3 trials at 6 different maximum torque levels, from 0.5N-m to 3.0 N-m at every half N-m interval. Instead of using LabView and the DAQ setup, we were able to program the microcontroller to take data that could then be exported to a CSV file afterwards. The testing was difficult because the best way to align the Instron data and strain data was to push the buttons at the same time. However, shortly into the testing we realized that the strain data was on a bit of a delay and as a result we needed to start the Instron slightly after we started collecting the strain data. Figures 23 and 24 are one trial of the torque vs. time graph obtained from the Instron and the strain vs. time graph obtained from the microcontroller.

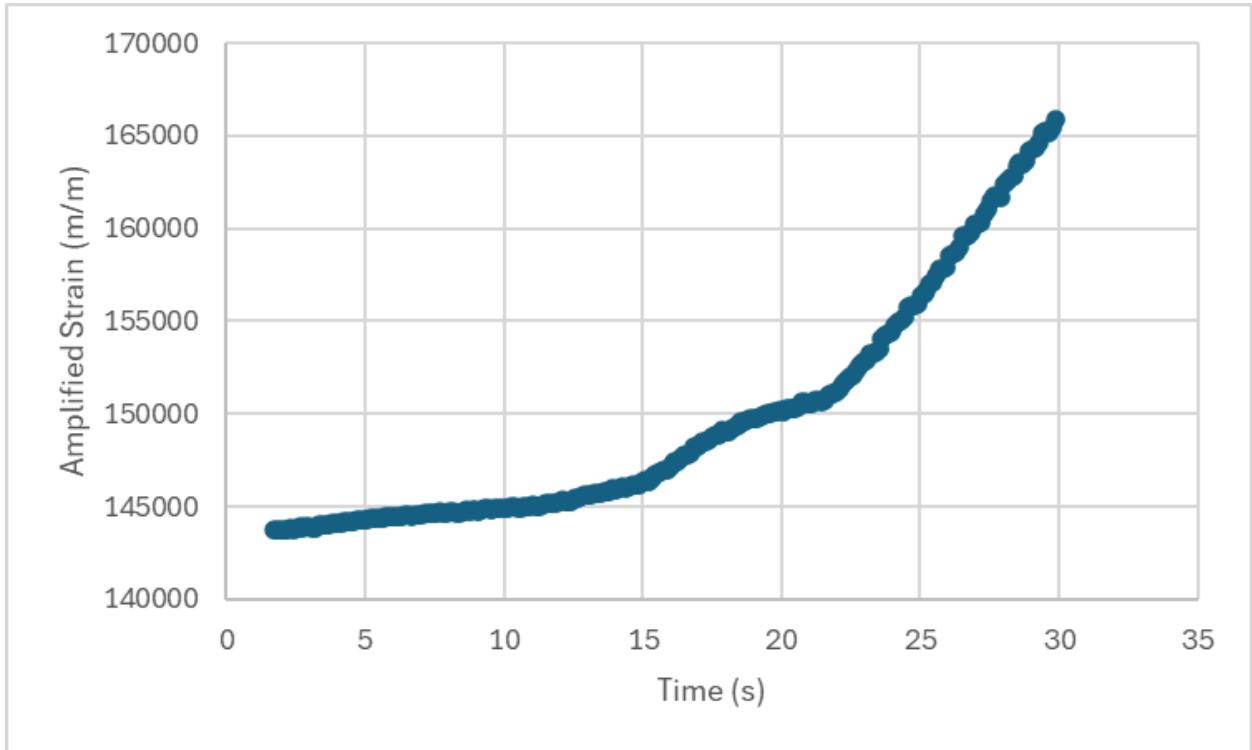


Figure 23: Amplified Strain vs. Time for one trial at 1.5 N-m

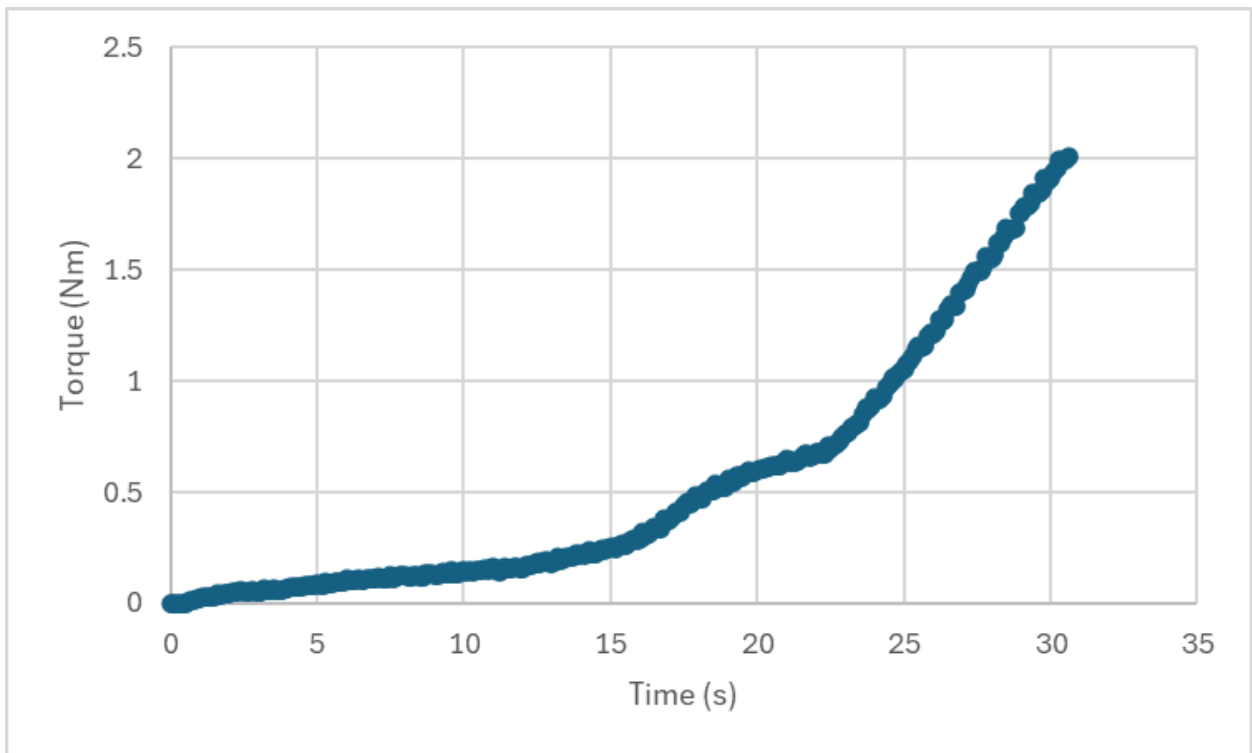


Figure 24: Torque vs. Time graph for same 1.5 N-m

After we had both sets of CSV files, we wrote a MATLAB function, as seen in Appendix C, that would parse through the CSV files and align the times between them. The microcontroller data started around 1.6 seconds each time, so the function had to shift all of the data to account for that. Additionally, the microcontroller was supposed to take data every 0.1 seconds, but was on a slight delay. As a result, the function needed to get rid of the torque values to make sure there were the same number of strain and torque data points. Figure 25 shows the averages of the three trials at each of the different torque intervals. The strain values on the x-axis are divided by a constant of 140,000, which correlates to approximately zero from the amplifier.

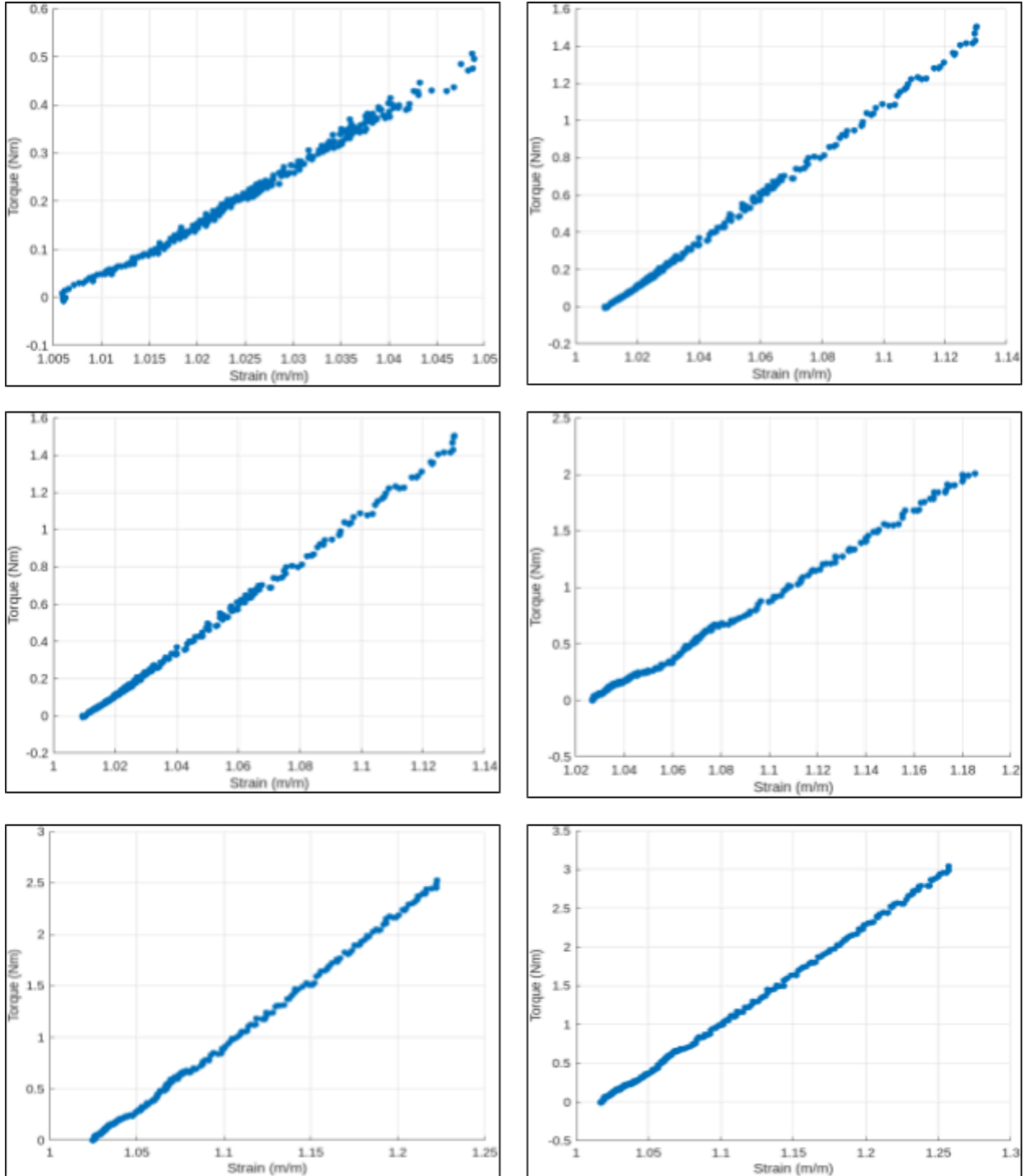


Figure 25: Torque vs. Strain for Final Instron Testing at 0.5 N-m (Upper-Left), 1.0 N-m (Upper-Right), 1.5 N-m (Middle-Left), 2.0 N-m (Middle-Right), 2.5 N-m (Lower-Left), and 3.0 N-m (Lower-Right)

After graphing all of the averages from the MATLAB function, we were able to obtain a line of best fit for the relationship between torque and strain, as seen in Figure 26. For the slope of the line of best fit, we divided by the constant of 140,000. As seen on the graph, the R^2 value was very high at 0.9823, which was good, as we expected the strain to increase proportionally to the torque. Although our R^2 value was high, we concluded that we could accurately measure the torque to within ± 0.18 N-m. This value was not acquired from error propagation because the amplifier was 24-bit ADC, and if we used the least-significant bit method we would get an error on a nanoscale level. Although this error may be true, we concluded that there should be a larger error because of the timing discrepancy between the two systems. As a result, we determined the 0.18 N-m from plugging in the strain values associated with the maximum torque from each trial and compared it to the torque given by the Instron. The torque from the relationship with the largest difference to the Instron torque was 0.18 N-m.

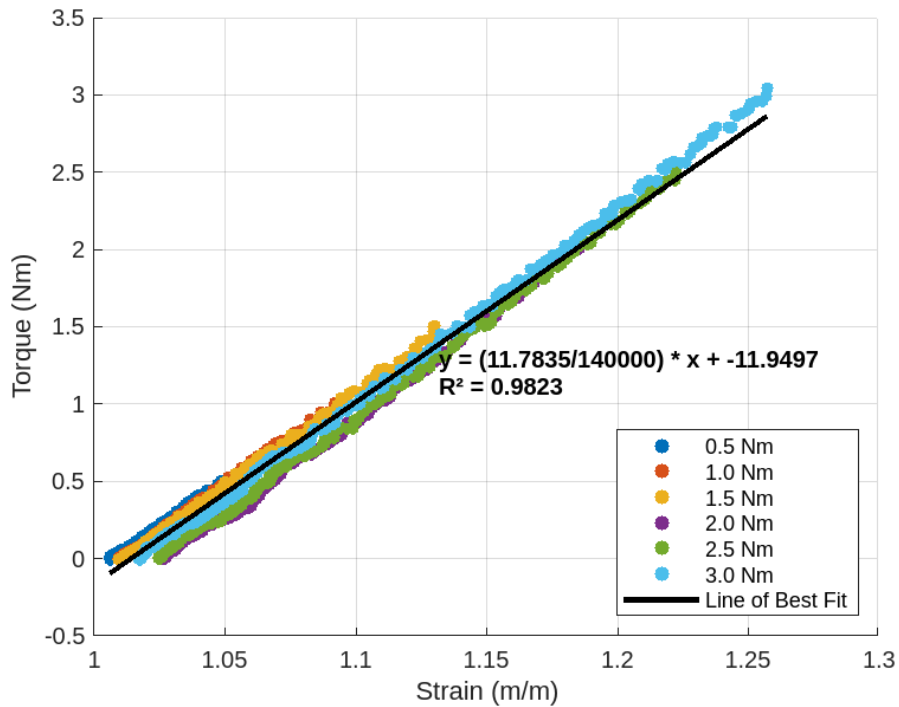


Figure 26: Final Average Graph Torque vs. Strain with Line of Best and Error

Final Device Testing - Wood and Bone

After assembling the final prototype and verifying the results on the instron machine, it was time to conduct tests with the device attached to a drill. First, we conducted testing on two different wood samples, as we had previously done in our early testing. The maple wood, which is more dense, showed similar results to the data we gathered from our previous testing. Similarly, the less dense pine was below the line for maple, requiring less torque for the same amount of axial force. Figure 27 shows how the device verified it was giving us reliable data that mirrored what we saw in our previous testing with the wood samples.

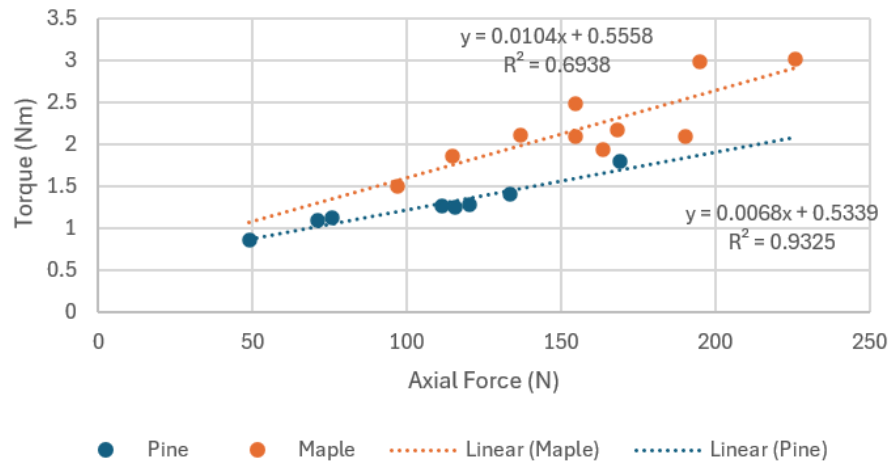


Figure 27: Torque vs. Axial Force for Pine and Maple (Final Testing)

Following this, we conducted testing on bones from a Highland Cow, which are shown in Figure 28. In order to test if our device could tell the difference between high strength and low strength bone, we focused on testing at the midpoint and endpoints of the femur bone. The internal bone structure is such that the ends of the bone have a much thicker outer layer of hard bone. Whereas the midpoint is much thinner, resulting in a low strength fixation point. As can be seen in Figure 29, the two holes drilled at the end points of the femur resulted in torque values between 1 N-m and 1.2 N-m. Conversely, the three holes drilled in the middle were significantly

lower, roughly 0.6 N-m. This data was very promising, highlighting that our device could give consistent, reliable results while also identifying strong and weak points in the bone samples.

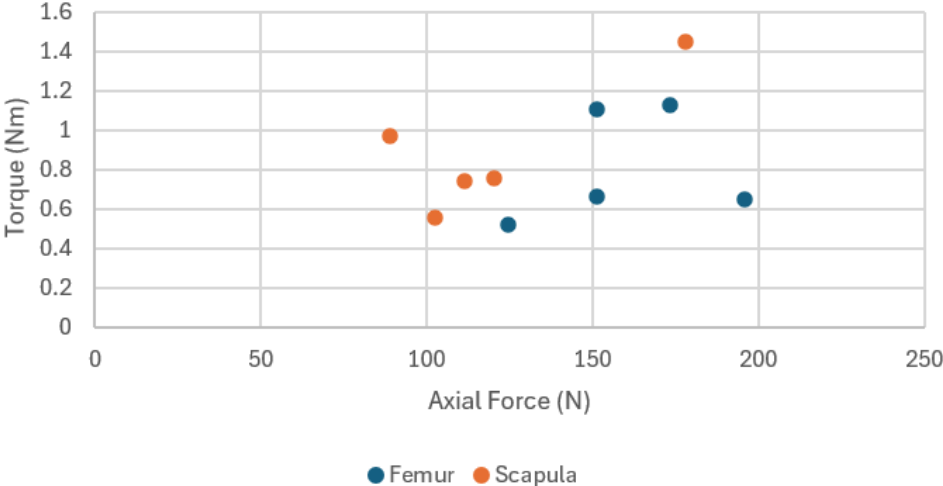


Figure 28: Torque vs. Axial Force for Highland Cow Bone Testing



Figure 29: Highland Cow Femur (Left) and Scapula (Right) Bone Testing

Final Specifications and Design Outcomes

Finally, the initial specifications were refined to account for the changes and iteration that occurred throughout the development process. Some of the initial specifications were removed, as they were unattainable given the time and resources provided to us. The final specifications that our device meets are bolded below, and an explanation of how our device did or did not meet these specifications is provided under each.

1. The device should be sensitive to small changes in torque.
 - a. Ensure the load cell and strain gauges pick up small differences in bone strength.

The sampling rate must be large enough to detect different layers of the bone.

 - i. **Marginal Value: 0.2 N-m**
 - ii. Ideal Value: 0.02 N-m

→ *The margin of error for the torque measurements is ± 0.18 N-m. Thus, the device is sensitive enough to meet the marginal value, but not the ideal value.*
2. The device should be easily attached and removed from the surgical drill.
 - a. Measure the amount of time it takes users to add and remove the device and ensure it does not hinder the user.
 - i. **Marginal Value: 10 seconds**
 - ii. **Ideal Value: 5 seconds**

→ *The device can be easily attached within 5 seconds to a standard handheld drill. This ease of attachment will carry over to surgical drills.*
3. The device must take real-time measurements.
 - a. The device should update its measurements over a short period of time without a noticeable lapse.

i. Marginal Value: 100 Hz

ii. Ideal Value: 500 Hz

→ *The device has the ability to take measurements at a high frequency, however, due to the limited memory on the microcontroller and in order to compare the data to our Instron testing, we set the frequency at 10 Hz. Since this device has the ability to take real-time measurements at 500 Hz, we believe the device meets the ideal value.*

4. The device must not decrease the torque of the handheld drill.

a. Look up in the user's manual the maximum torque the drill is supposed to reach. Measure the maximum torque after the device is attached using the device and make sure they are within.

i. Marginal Value: 5%

ii. Ideal Value: 2%

→ *The device does not noticeably decrease the torque of the drill. Testing was conducted on specimens that were not dense enough to reach the drill's maximum torque. Since the device did not decrease the torque of the drill during each trial, we believe the specification is met.*

5. The device must account for the axial force that is applied while drilling.

a. Determine the relationship between applied torque and axial force through testing, which will be used to offset the readings.

i. Marginal Value: Yes

ii. Ideal Value: Yes

→ *Although we determined that axial force is a necessary consideration, we were not able to include this consideration in our device due to time constraints. We instead decided to focus on measuring torque, as this proved to be more difficult than originally thought.*

6. The device must be able to accurately estimate the local bone strength of animal bones

a. Determine the density of animal bones by measuring the mass and volumetric water displacement. Through the relationship we derived, measure the bone density using our device and ensure that it is within.

i. **Marginal Value: 20%**

ii. **Ideal Value: 10%**

→ *We were unable to accurately measure the density of animal bones using water displacement or CT/DEXA scans. Instead, we decided to focus on the proof of concept for drilling into animal bones and detecting changes in general strength.*

7. The device must be of a reasonable size, shape, and mass to not interfere with normal drill usage.

a. The volume and mass of the device is within ___ of current surgical drills.

i. **Marginal Value: 20%**

ii. **Ideal Value: 10%**

→ *While the mass is within 20%, the volume of our device did not meet this marginal value. Neither metric meets the ideal value of 10%.*

8. The device should output data in a readable format and save it for later review.

a. Ensure the output is easily readable and ensure that the saved output does not lose any data.

i. Marginal Value: Yes

ii. Ideal Value: Yes

→ *The data from this device can be output to a CSV file and saved for later review.*

9. The drill bit must remain securely attached to the device during operation.

a. Ensure the bit does not loosen or fall out while holding the device downwards and shaking it. Take a slow-motion video of the device to test before drilling into a material.

i. Marginal Value: Yes

ii. Ideal Value: Yes

→ *Set screws were utilized to properly secure the drill bit to the device. There is no discernable movement of the drill bit during use.*

10. The load cell internal structure must strain at a rate that the strain gauges can detect.

a. Use FEA to determine the strain for given load cell geometries and ensure that is within the range of the strain gauges.

i. Marginal Value: Yes

ii. Ideal Value: Yes

→ *FEA was conducted to determine the magnitude of strain for the load cell, and this value is within the range of the specifications of the strain gauges used. The device detects measurable changes in strain.*

Summary and Conclusions

Overall, we found success in producing a reasonable proof of concept relating torque to density in real time. Measuring strain allowed for a great approximation in the torque changes, and therefore the coinciding strength variations. Similarly, the microcontroller was a valuable contribution, as it was able to display the torque changes in a clear and accurate manner through the RGB LED. However, there are several necessary additions needed before it is ideal for an orthopedic procedure. Firstly, the axial force must be considered because it greatly affects the torque output, as proven by the initial testing. Originally, the prototype was supposed to account for this by having two adhesive force sensors on the drill handle, but time constraints prevented this implementation. Additionally, the final prototype is strictly Jacobs chuck compatible and not able to connect to Stryker medical drills. Therefore, the ends need to be re-machined in order to attach to the quick connect device that 90% of surgical drills utilize. Furthermore, the original parameters required the prototype to have a real-time data display for the surgeons to reference mid-procedure. The strain data can be saved to a CSV file after the fact, but requires manual input from the user by pressing a button. With a higher budget, we could purchase more advanced electronics equipped with wireless transmission, allowing the data to be relayed to a nearby display in real-time. Finally, the overall structure of the design can be improved, both in its size and organization. It is much too large to be actually used in surgery, as it would not fit into tight environments. Similarly, the external components and accompanying wiring prevents sterilization and water resistance, two qualities necessary for this device to be used during surgical procedures.

Appendix A: References

- Fogelman, I., & Blake, G. M. (2000). Different Approaches to Bone Densitometry. *Journal of Nuclear Medicine*, 41(12), 2015–2025. <https://jnm.snmjournals.org/content/41/12/2015>
- Gilmer, B. B., & Lang, S. D. (2018). Dual Motor Drill Continuously Measures Drilling Energy to Calculate Bone Density and Screw Pull-out Force in Real Time. *Journal of the American Academy of Orthopaedic Surgeons. Global research & reviews*, 2(9), e053. <https://pmc.ncbi.nlm.nih.gov/articles/PMC6226295/>
- Kushchayeva, Y., Pestun, I., Kushchayev, S., Radzikhovska, N., & Lewiecki, E. M. (2022). Advancement in the Treatment of Osteoporosis and the Effects on Bone Healing. *Journal of Clinical Medicine*, 11(24), 7477. <https://doi.org/10.3390/jcm11247477>
- Johns Hopkins Medicine. (n.d.). *Bone densitometry*. <https://www.hopkinsmedicine.org/health/treatment-tests-and-therapies/bone-densitometry>
- National Institute of Arthritis and Musculoskeletal and Skin Diseases (NIAMS). (n.d.). *Bone mineral density tests: What the numbers mean*. U.S. Department of Health and Human Services. Retrieved December 8, 2024, from <https://www.niams.nih.gov/health-topics/bone-mineral-density-tests-what-numbers-mean>

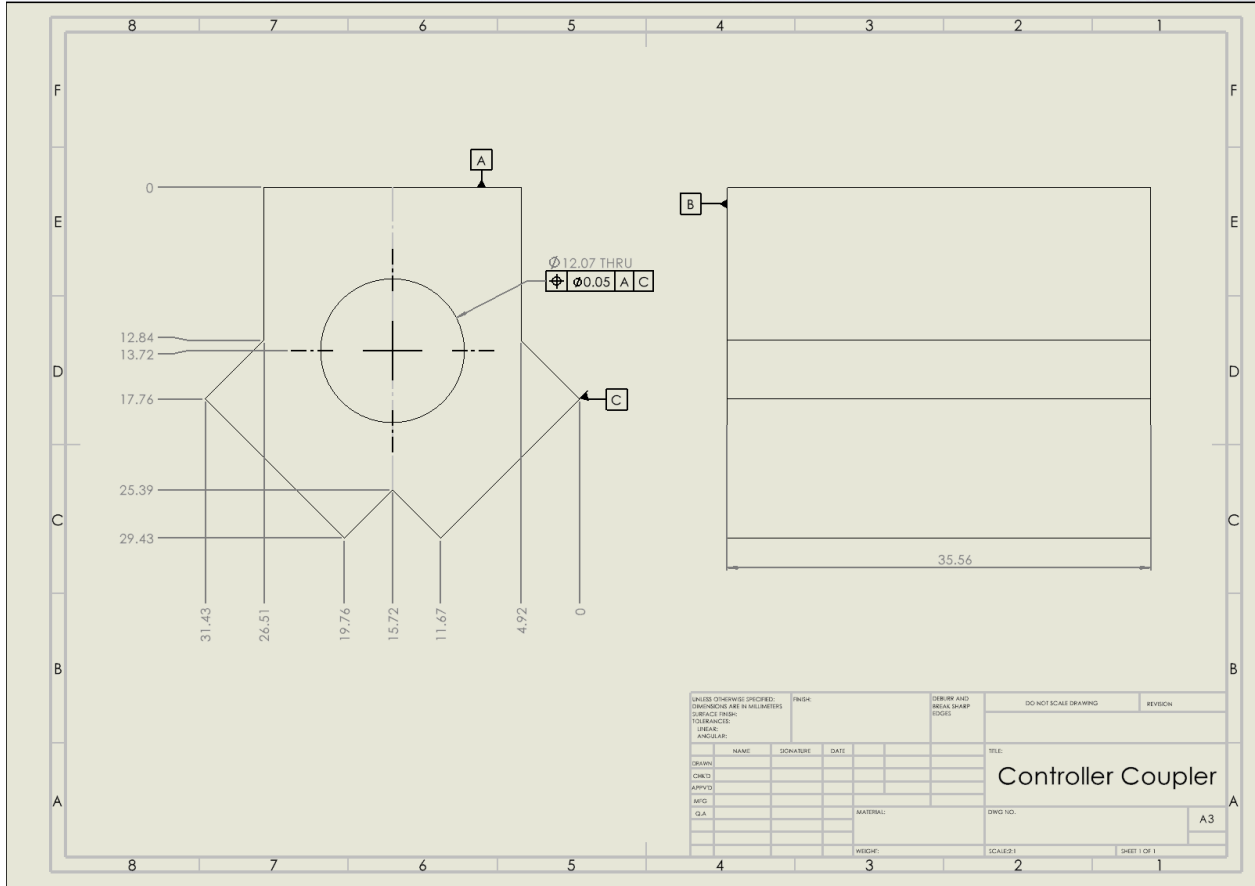


Figure 32: Controller Coupler Drawing

Appendix C: Code

```
1 import time
2 import board
3 import digitalio
4 import adafruit_dotstar # type: ignore
5 import os
6
7 # Define HX711 pins and LED
8 DATA_PIN = board.D2 # Data pin
9 CLOCK_PIN = board.D3 # Clock pin
10 led = adafruit_dotstar.DotStar(board.APA102_SCK, board.APA102_MOSI, 1)
11 led.brightness = 0.3
12
13 # Initialize pins
14 data = digitalio.DigitalInOut(DATA_PIN)
15 data.direction = digitalio.Direction.INPUT
16 clock = digitalio.DigitalInOut(CLOCK_PIN)
17 clock.direction = digitalio.Direction.OUTPUT
18
19 def read_hx711():
20     """Reads a 24-bit value from the HX711."""
21     while data.value: # Wait for HX711 to be ready (DATA_PIN == 0)
22         pass
23
24     value = 0
25     for i in range(24):
26         clock.value = True
27         value = (value << 1) # Shift left and read next bit
28         clock.value = False
29         if data.value:
30             value+=1
31
32     # Send 3 more pulses to set gain 'Set Gain (1=128, 2=32, 3=64)
33     for i in range(3):
34         clock.value = True
35         clock.value = False
36     return value
37
38 def write_csv(timestamp, reading):
39     try:
40         with open("/strain_data.csv", "a") as f:
41             f.write(f"{timestamp},{reading}\n")
42     except OSError as e:
43         print("Write failed:", e)
44
45 # Add header if file doesn't exist
46 if "strain_data.csv" not in os.listdir("/"):
47     with open("/strain_data.csv", "w") as f:
48         f.write("time,reading\n")
49
50 # Main loop
51 count = 0
52 while True:
53     strain_value = read_hx711()
54     timestamp = time.monotonic()
55
56     # Print and log data
57     print(f"Strain Gauge Reading {count} = {strain_value} at {timestamp:.2f}s")
58     write_csv(timestamp, strain_value)
59
60     # LED color logic
61     if strain_value > 160000:
62         led[0] = (0, 255, 0) # Green: High strain
63     elif strain_value > 150000:
64         led[0] = (255, 255, 0) # Yellow: Medium strain
65     else:
66         led[0] = (255, 0, 0) # Red: Low strain or no load
67
68     count+=1
69     time.sleep(.1) # Wait 0.1 seconds
```

Figure 33: Trinket M0 Python Program

```

MATLAB Drive/getSlopeIntercept1.m
1 function [slope, intercept, x_reg, y_reg] = getSlopeIntercept1(filename, sheet, makePlot)
2 % getSlopeIntercept - Computes linear regression slope and intercept from a specified sheet
3 %
4 % Inputs:
5 % filename - Excel file name (e.g., 'WorkingStrainData.xlsx')
6 % sheet - Sheet name or index to process (e.g., 'Sheet2')
7 % makePlot - Boolean (true/false) to control plotting
8 %
9 % Outputs:
10 % slope - Slope of the linear regression
11 % intercept - Intercept of the linear regression
12 % x_reg - x-values used in regression (interpolated B)
13 % y_reg - y-values used in regression (from column D)
14
15 % Read data from the specified sheet
16 data = readmatrix(filename, 'Sheet', sheet);
17
18 % Extract columns B, C, D, and E
19 colB = data(:, 2); % y-values to interpolate
20 colC = data(:, 3); % x-values for interpolation (original x)
21 colD = data(:, 4); % desired new x-axis for plotting
22 colE = data(:, 5); % associated data, and defines target length
23
24 % Clean data: only keep non-NaN from B and C
25 validBC = ~isnan(colB) & ~isnan(colC);
26 x = colC(validBC);
27 y = colB(validBC);
28
29 % Count non-NaN entries in column E
30 nE = sum(~isnan(colE));
31
32 % Interpolation points (based on original x's range)
33 x_interp = linspace(min(x), max(x), nE);
34
35 % Interpolate y-values (new B)
36 y_interp = interp1(x, y, x_interp, 'linear');
37
38 % Extract first nE valid rows from columns D and E
39 validDE = ~isnan(colD) & ~isnan(colE);
40 colD_clean = colD(validDE);
41 colE_clean = colE(validDE);
42 colD_trim = colD_clean(1:nE);
43 colE_trim = colE_clean(1:nE);
44
45 % Combine into a matrix: [x_interp, y_interp, colE_trim, colD_trim]
46 fullData = [x_interp', y_interp'/140000, colE_trim, colD_trim];
47
48 % Flip axes: Interpolated B as x, D as y
49 x_reg = fullData(:, 2); % Interpolated B (now x)
50 y_reg = fullData(:, 4); % D column (now y)
51
52 % Linear regression
53 p = polyfit(x_reg, y_reg, 1);
54 slope = p(1);
55 intercept = p(2);
56
57 % Print results
58 fprintf('Sheet "%s": y = %.4f * x + %.4f\n', sheet, slope, intercept);
59
60 % Optional plot
61 if makePlot
62     figure;
63     plot(x_reg, y_reg, 'bo'); hold on;
64     plot(x_reg, polyval(p, x_reg), 'r-', 'LineWidth', 2);
65     xlabel('Interpolated B (x-axis)');
66     ylabel('D (y-axis)');
67     title(['Linear Regression for ', sheet]);
68     legend('Data', 'Fitted Line', 'Location', 'southeast');
69     grid on;
70 end
71 end

```

Figure 34: MATLAB Code

Appendix D: Assembly Drawing and Parts List

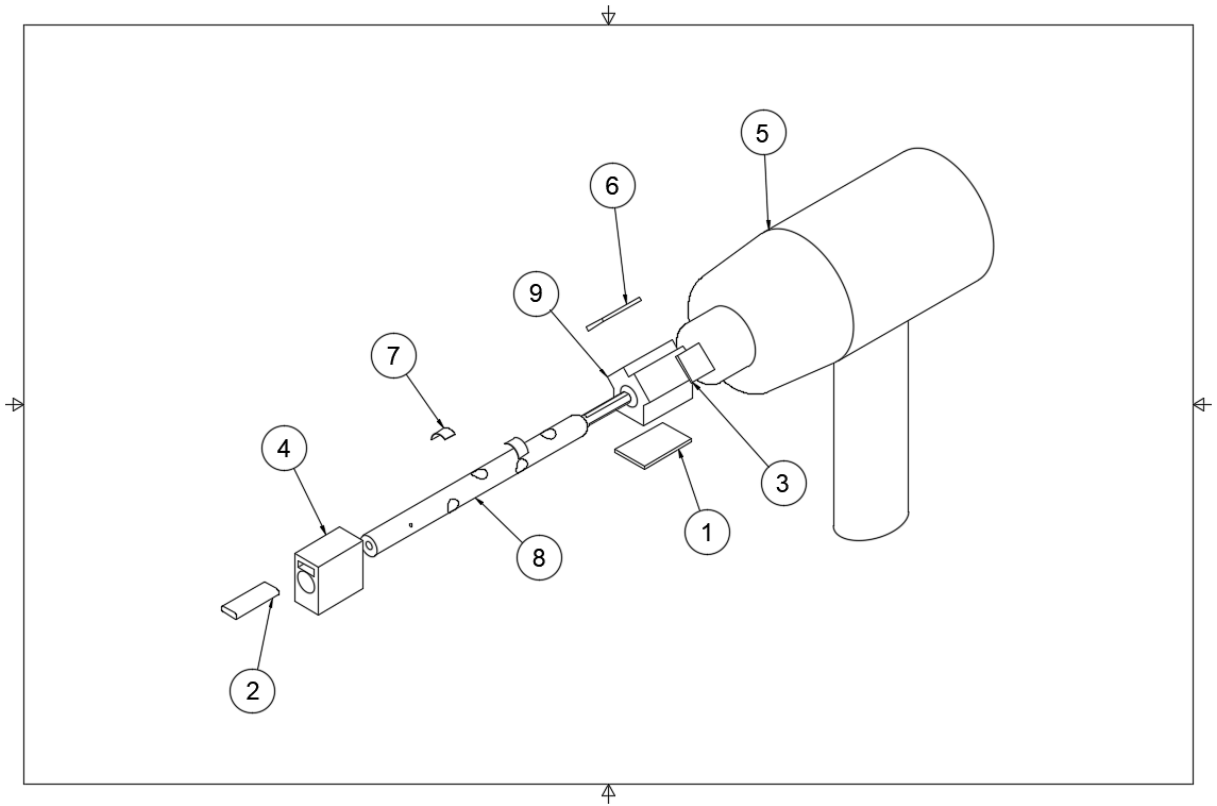


Figure 35: Assembly Drawing

Table 2: Parts List

Number	Quantity	Part Name
1	1	HX711 Load Cell Amplifier
2	1	3.3V Lithium Ion Polymer Battery
3	1	Adafruit LiPoly Backpack Add-On
4	1	Battery Coupler
5	1	Cordless Drill
6	1	Adafruit Trinket M0 Microcontroller
7	2	Rosette Strain Gauges
8	1	Custom Load Cell Shaft
9	1	Electronic Component Coupler